Incorporation of Group 11 Metal Ions into a Diplatinum Center Leading to Pt_2M Heterotrinuclear Complexes Supported by a Tridentate Phosphine Ligand (M = Au, Ag, Cu)

Tomoaki Tanase,*,† Hirotaka Toda, and Yasuhiro Yamamoto*

Department of Chemistry, Faculty of Science, Toho University, Miyama 2-2-1, Funabashi, Chiba 274, Japan

Received June 27, 1996[⊗]

The reaction of *syn*-$[Pt_2(\mu\text{-dpmp})_2(XylNC)_2](PF_6)_2$ (**1**) with $AuPF_6$ yielded the Pt_2Au trinuclear complex $[Pt_2Au(\mu\text{-dpmp})_2(XylNC)_2](PF_6)_3$ (**7**) in 60% yield. The structure was determined by X-ray crystallography to comprise a Pt_2Au trinuclear core bridged by two dpmp ligands (**7**·$(CH_3)_2CO$: monoclinic, *P2₁/n* (No. 14), $a = 15.147(3)$ Å, $b = 25.947(8)$ Å, $c = 25.759(6)$ Å, $\beta = 104.10(2)°$, $V = 9818$ Å^3, $Z = 4$, $D_{calcd} = 1.593$ g cm^{-3}, $R = 0.065$, and $R_w = 0.059$). An Au(I) ion is trapped by two uncoordinated phosphine units in **1** to lead a deformed Pt−Pt−Au aggregation. The Pt−Pt and Pt···Au distances are 2.708(2) and 3.045(2) Å, respectively, and the Pt−Pt···Au angle is 110.68(5)°. The similar Pt_2Ag cluster, $[Pt_2Ag(\mu\text{-dpmp})_2(XylNC)_2](PF_6)_3$ (**8**), was also prepared by the reaction of complex **1** with $AgPF_6$ in 70% yield. The crystal structure is essentially identical to that of **7** (monoclinic, *C2/c* (No. 15), $a = 18.302(6)$ Å, $b = 25.056(6)$ Å, $c = 47.172(9)$ Å, $\beta = 99.11(3)°$, $V = 21359$ Å^3, $Z = 8$, $D_{calcd} = 1.373$ g cm^{-3}, $R = 0.089$, and $R_w = 0.078$). The Pt−Pt and Pt···Ag distances are 2.657(2) and 3.118(3) Å, respectively, and the Pt−Pt···Ag angle is 136.36(8)°. Reactions of **1** with CuX (X = I, Br, Cl) gave yellow complex $[Pt_2CuX(\mu\text{-dpmp})_2(XylNC)_2](PF_6)_2$ (**9**, X = I; **10**, X = Br; **11**, X = Cl), in good yield (**9**·Et_2O: monoclinic, *P2₁/c* (No. 14), $a = 15.048(4)$ Å, $b = 21.922(3)$ Å, $c = 27.840(3)$ Å, $\beta = 101.89(1)°$, $V = 8987$ Å^3, $Z = 4$, $D_{calcd} = 1.641$ g cm^{-3}, $T = 23$ °C, $R = 0.056$, and $R_w = 0.046$. **10**·Et_2O: monoclinic, *P2₁/c* (No. 14), $a = 14.910(4)$ Å, $b = 21.891(7)$ Å, $c = 27.226(8)$ Å, $\beta = 101.66(6)°$, $V = 8702$ Å^3, $Z = 4$, $D_{calcd} = 1.658$ g cm^{-3}, $T = -95$ °C, $R = 0.042$, and $R_w = 0.046$. **11**·Et_2O: monoclinic, *P2₁/c* (No. 14), $a = 15.037(4)$ Å, $b = 22.081(6)$ Å, $c = 27.449(4)$ Å, $\beta = 101.92(2)°$, $V = 8917$ Å^3, $Z = 4$, $D_{calcd} = 1.585$ g cm^{-3}, $T = 23$ °C, $R = 0.040$, and $R_w = 0.041$). The Pt_2CuX assembly forms a rhombic structure with the Pt−Pt, Pt···Cu, Cu−X, and Pt···X distances being 2.715−2.727, 2.857−2.872, 2.276−2.597, and 3.088−3.130 Å, respectively. The CuI fragment is trapped by the pendant phosphorus arms of **1**. The Pt···Cu−X angle is interestingly less than 90°, resulting in a relatively short interatomic distance between the terminal Pt and X atoms. A monovalent group 11 metal ion (Au(I), Ag(I), or Cu(I)), which has a d^{10} configuration, was readily incorporated into the Pt_2 core, leading to a heterotrimetallic Pt_2M aggregation.

Introduction

Heterometallic di-, tri-, and tetranuclear complexes, so-called small-size clusters, have attracted increasing attention owing to their potential to promote new catalytic reactions which are no longer established by each mononuclear system and to be minimal models for mixed-metal heterogeneous catalysts as well as photochemical devices.[1] The arrangements of metal centers could be designed by a choice of supporting ligand such as multidentate phosphines. A variety of heterodimetallic centers has been studied by utilizing bis(diphenylphosphino)methane and 2-(diphenylphosphino)pyridine,[2,3] and recently, Balch and co-workers have developed a series of MM′M heterotrinuclear systems with 2,6-bis(diphenylphosphino)pyridine and bis-((diphenylphosphino)methyl)phenylarsine.[4,5] We have recently started to use the triphosphine ligand, bis((diphenylphosphino)-methyl)phenylphosphine (dpmp)[5,6] in our platinum and palladium cluster chemistry[7] and have reported that the reaction of $[Pt_2(XylNC)_6](PF_6)_2$ (Xyl = 2,6-dimethylphenyl) with dpmp

†Present address: Department of Chemistry, Faculty of Science, Nara Women's University, Kitauoya-higashi-machi, Nara 630, Japan.

⊗ Abstract published in *Advance ACS Abstracts,* March 1, 1997.

(1) (a) Roberts, D. A.; Geoffroy, G. L. In *Comprehensive Organometallic Chemistry*; Wilkinson, G., Stone, F. G. A., Eds.; Pergamon: Oxford, U.K., 1982; Vol. 6, Chapter 40. (b) Muetterties, E. L.; Kause, M. J. *Angew. Chem., Int. Ed. Engl.* **1983**, *22*, 135. (c) Stephan, D. W. *Coord. Chem. Rev.* **1989**, *95*, 41.

(2) (a) Puddephatt, R. J. *Chem. Soc. Rev.* **1983**, *12*, 99. (b) Balch, A. P. In *Homogeneous Catalysis with Metal Phosphine Complexes*; Pignolet, L. H., Ed.; Plenum Press: New York, 1983; p 167. (c) Chaudret, B.; Delavaux, B.; Poilblanc, R. *Coord. Chem. Rev.* **1988**, *86*, 191.

(3) (a) Puddephatt, R. J.; Manojlovic-Muir, L.; Muir, K. W. *Polyhedron* **1990**, *9*, 2767, and references cited therein. (b) Payne, N. C.; Ramachandran, R.; Schoettel, G.; Vittal, J. J.; Puddephatt, R. J. *Inorg. Chem.* **1991**, *30*, 4048. (c) Jennings, M. C.; Schoettel, G.; Roy, S.; Puddephatt, R. J. *Organometallics* **1991**, *10*, 580. (d) Xiao, J.; Vittal, J. J.; Puddephatt, R. J. *J. Am. Chem. Soc.* **1993**, *115*, 7882. (e) Xiao, J.; Puddephatt, R. J. *J. Am. Chem. Soc.* **1994**, *116*, 1129. (f) Xiao, J.; Hao, L.; Puddephatt, R. J. *Organometallics* **1995**, *14*, 2194.

(4) (a) Balch, A. L. *Pure Appl. Chem.* **1988**, *60*, 555. (b) Balch, A. L.; Hope, H.; Wood, F. E. *J. Am. Chem. Soc.* **1985**, *107*, 6936. (c) Balch, A. L.; Fossett, L. A.; Plmstead, M. M.; Reedy, P. E., Jr. *Organometallics* **1986**, *5*, 1929. (d) Balch, A. L.; Ghedini, M.; Oram, D. E.; Reedy, P. E., Jr. *Inorg. Chem.* **1987**, *26*, 1223. (e) Bailey, D. A.; Balch, A. L.; Fossett, L. A.; Olmstead, M. M.; Reedy, P. E., Jr. *Inorg. Chem.* **1987**, *26*, 2413. (f) Balch, A. L.; Fosset, L. A.; Olmstead, M. M.; Reedy, P. E., Jr. *Organometallics* **1988**, *7*, 430. (g) Balch, A. L.; Olmstead, M. M.; Neve, F.; Ghedini, M. *New J. Chem.* **1988**, *12*, 529. (h) Balch, A. L.; Nagle, J. K.; Oram, D. E.; Reedy, P. E., Jr. *J. Am. Chem. Soc.* **1988**, *110*, 454. (i) Bailey, D. A.; Balch, A. L.; Davis, B. J.; Neve, F.; Olmstead, M. M. *Organometallics* **1989**, *8*, 1000. (j) Balch, A. L.; Davis, B. J.; Olmstead, M. M. *Inorg. Chem.* **1989**, *28*, 3148. (k) Balch, A. L.; Olmstead, M. M.; Pram, D. E.; Reedy, P. E., Jr.; Reimer, S. H. *J. Am. Chem. Soc.* **1989**, *111*, 4021. (l) Balch, A. L.; Ctalano, V. J.; Noll, B. C.; Olmstead, M. M. *J. Am. Chem. Soc.* **1990**, *112*, 7558. (m) Balch, A. L.; Fung, E. Y.; Olmstead, M. M. *Inorg. Chem.* **1990**, *29*, 3203. (n) Balch, A. L.; Catalano, V. J.; Chatfield, M. A.; Nagle, J. K.; Olmstead, M. M.; Reedy, P. E., Jr. *J. Am. Chem. Soc.* **1991**, *113*, 1252. (o) Balch, A. L.; Neve, F.; Olmstead, M. M. *J. Am. Chem. Soc.* **1991**, *113*, 2995.

S0020-1669(96)00771-9 CCC: $14.00

Scheme 1

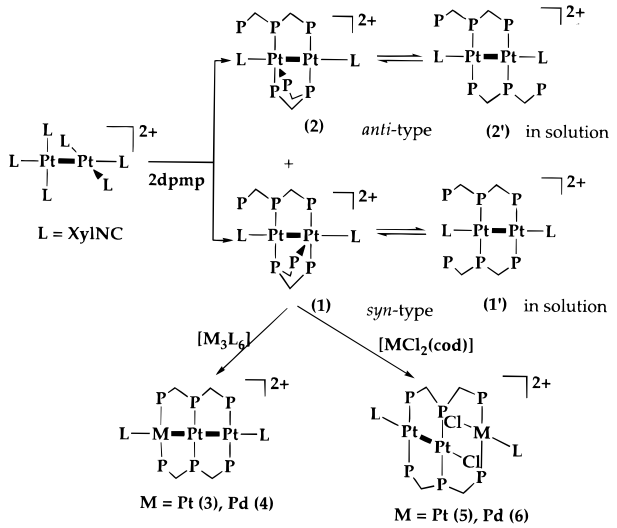

afforded a mixture of isomeric diplatinum complexes, *syn*- and *anti*-$[Pt_2(\mu\text{-dpmp})_2(XylNC)_2](PF_6)_2$ (**1** and **2**), where the central P atoms of the dpmp ligands bind to the same metal center in **1** (*syn*-type) and to the different metal centers in **2** (*anti*-type) (Scheme 1).[8] Complexes **1** and **2** are fluxional in solution *via* the symmetrical structures **1′** and **2′** and are regarded as good precursors of homo- and heterometallic small-sized clusters because they have uncoordinated phosphine units. In particular, the *syn*-$[Pt_2(\mu\text{-dpmp})_2(XylNC)_2](PF_6)_2$ (**1**) was readily transformed, by treatment with $[M_3(XylNC)_6]$, to linear homo- and heterotrinuclear clusters, *linear*-$[Pt_2M(\mu\text{-dpmp})_2(XylNC)_2](PF_6)_2$ (**3**, M = Pt; **4**, M = Pd),[8] and, with $[M^{II}Cl_2(cod)]$, to combined dimer−monomer complexes, $[Pt_2M(\mu\text{-dpmp})_2(XylNC)_2](PF_6)_2$ (**5**, M = Pt; **6**, M = Pd).[9] These results suggested that the choice of additional metal ions could systematically tune the structures and properties of resultant trinuclear complexes. We report herein the reaction of **1** with monovalent group 11 metal ions, leading to Pt_2M heterotrinuclear complexes, where M = Au, Ag, Cu.

Experimental Section

Dichloromethane and acetone were distilled over calcium hydride and diethyl ether over lithium aluminum hydride prior to use. Other reagents were of the best commercial grade and were used as received. Complex *syn*-$[Pt_2(\mu\text{-dpmp})_2(XylNC)_2](PF_6)_2$ (**1**) was prepared by the methods already reported.[8,10] Compounds $[AuCl(PPh_3)]$,[11] $[Cu(CH_3CN)_4](PF_6)$,[12] bis((diphenylphosphino)methyl)phenylphosphine (dpmp),[13] and 2,6-xylyl isocyanide (XylNC)[14] were prepared by the known methods. All reactions were carried out under a nitrogen atmosphere with standard Schlenk and vacuum line techniques.

Measurement. ^1H NMR spectra were measured on a Bruker AC250 instrument at 250 MHz. Chemical shifts were calibrated to tetramethylsilane as an external reference. $^{31}P\{^1H\}$ NMR spectra were recorded by the same instrument at 101 MHz, chemical shifts being calibrated to 85% H_3PO_4 as an external reference. Infrared and electronic absorption spectra were recorded with Jasco FT/IR-5300 and Ubest-30 spectrometers, respectively.

Preparation of $[Pt_2Au(\mu\text{-dpmp})_2(XylNC)_2](PF_6)_3$ (7). Compounds *syn*-$[Pt_2(\mu\text{-dpmp})_2(XylNC)_2](PF_6)_2$ (**1**) (50.0 mg, 2.56×10^{-2} mmol), $[AuCl(PPh_3)]$ (13.3 mg, 2.69×10^{-2} mmol), and $NaPF_6$ (5.6 mg, 3.3×10^{-2} mmol) were dissolved in a dichloromethane (5 mL)/acetone (5 mL) mixed solvent, and the solution was stirred at room temperature for 16 h. The solvent was removed under reduced pressure, and the residue was crystallized from a acetone/diethyl ether mixed solvent to give yellow blocked-shape crystals of $[Pt_2Au(\mu\text{-dpmp})_2(XylNC)_2](PF_6)_3$ (**7**) in 60% yield (35.5 mg). Anal. Calcd for $C_{82}H_{76}N_2F_{18}P_9Pt_2Au$: C, 42.87; H, 3.33; N, 1.22%. Found: C, 42.72; H, 3.56; N, 1.28%. IR (Nujol): 2164, 2151 (N≡C), 837 (PF_6) cm^{-1}. ^1H NMR (acetone-d_6): δ 1.48 (s, *o*-Me), 1.54 (s, *o*-Me), 1.69 (s, *o*-Me), 1.70 (s, *o*-Me), 4.78, 5.48, 6.10 (m, CH_2), 6.8−8.7 (m, Ar). $^{31}P\{^1H\}$ NMR (acetone-d_6): δ −4.24 (m, $^1J_{PtP}$ = 2682 Hz, 1P), −2.31 (m, $^1J_{PtP}$ = 2331 Hz, 2P), 1.13 (m, $^1J_{PtP}$ = 2730 Hz, 1P), 33.34 (m, 2P). UV−vis (CH_2Cl_2; λ_{max} (log ϵ)): 364 (3.66) nm.

Preparation of $[Pt_2Ag(\mu\text{-dpmp})_2(XylNC)_2](PF_6)_3$ (8). To a dichloromethane solution (5 mL) of *syn*-$[Pt_2(\mu\text{-dpmp})_2(XylNC)_2](PF_6)_2$ (**1**) (52.5 mg, 2.68×10^{-2} mmol) was added $AgPF_6$ (10.2 mg, 4.03×10^{-2} mmol) dissolved in acetone (5 mL). The solution was stirred at room temperature for 6 h. The solvent was removed under reduced pressure, and the residue was crystallized from a dichloromethane/diethyl ether mixed solvent to give yellow crystals of $[Pt_2Ag(\mu\text{-dpmp})_2(XylNC)_2](PF_6)_3 \cdot CH_2Cl_2$ (**8**) in 70% yield (43.2 mg). Anal. Calcd for $C_{83}H_{78}N_2F_{18}P_9Pt_2AgCl_2$: C, 43.47; H, 3.43; N, 1.22%. Found: C, 43.64; H, 3.49; N, 1.31%. IR (Nujol): 2178, 2133 (N≡C), 841 (PF_6) cm^{-1}. ^1H NMR (acetone-d_6): δ 1.48 (s, *o*-Me), 1.64 (s, *o*-Me), 1.73 (s, *o*-Me), 1.73 (s, *o*-Me), 4.35, 5.15, 6.40 (m, CH_2), 6.8−8.5 (m, Ar). UV−vis (CH_2Cl_2; λ_{max} (log ϵ)): 308^{sh} (3.97) nm. Blocked-shape crystals suitable for X-ray crystallography were obtained by recrystallization of **8** from a acetone/diethyl ether mixed solvent at room temperature.

Preparation of $[Pt_2CuX(\mu\text{-dpmp})_2(XylNC)_2](PF_6)_2$ (X = I (9), Br (10), Cl (11)). Compounds *syn*-$[Pt_2(\mu\text{-dpmp})_2(XylNC)_2](PF_6)_2$ (**1**) (50.0 mmol, 2.56×10^{-2} mmol) and CuI (5.8 mg, 3.1×10^{-2} mmol) were dissolved in a two-layer solvent of dichloromethane (5 mL) and water (5 mL), and the resultant mixture was vigorously stirred at room temperature for 18 h. The dichloromethane layer was separated and dried over Na_2SO_4. The solvent was removed under reduced pressure after being passed through a glass filter, and the residue was crystallized from a acetone/diethyl ether mixed solvent to give yellow prismatic crystals of $[Pt_2CuI(\mu\text{-dpmp})_2(XylNC)_2](PF_6)_2$ (**9**) in 54% yield (29.6 mg). Anal. Calcd for $C_{82}H_{76}N_2F_{18}P_9Pt_2CuI$: C, 45.90; H, 3.57; N, 1.31%. Found: C, 45.77; H, 3.69; N, 1.33%. IR (Nujol): 2170, 2133

(5) Balch, A. L. *Prog. Inorg. Chem.* (Lippard, S. J., Ed.) **1994**, *41*, p 239.
(6) (a) Guimerans, R. R.; Olmstead, M. M.; Balch, A. L. *J. Am. Chem. Soc.* **1983**, *105*, 1677. (b) Olmstead, M. M.; Guimerans, R. R.; Balch, A. L. *Inorg. Chem.* **1983**, *22*, 2473. (c) Olmstead, M. M.; Guimerans, R. R.; Farr, J. P.; Balch, A. L. *Inorg. Chim. Acta* **1983**, *75*, 199. (d) Balch, A. L.; Guimerans, R. R.; Olmstead, M. M. *J. Organomet. Chem.* **1984**, *268*, C38. (e) Balch, A. L.; Fossett, L. A.; Guimerans, R. R.; Olmstead, M. M. *Organometallics* **1985**, *4*, 781. (f) Balch, A. L.; Guimerans, R. R.; Linehan, J. *Inorg. Chem.* **1985**, *24*, 290. (g) Balch, A. L.; Linehan, J. C.; Olmstead, M. M. *Inorg. Chem.* **1986**, *25*, 3937. (h) Balch, A. L.; Fossett, L. A.; Olmstead, M. M. *Organometallics* **1987**, *6*, 1827. (i) Balch, A. L.; Fossett, L. A.; Linehan, J.; Olmstead, M. M. *Organometallics* **1990**, *5*, 1638. (j) Balch, A. L.; Davis, B. J.; Olmstead, M. M. *Inorg. Chem.* **1990**, *29*, 3066. (k) Balch, A. L.; Catalano, V. J.; Olmstead, M. M. *J. Am. Chem. Soc.* **1990**, *112*, 2010. (l) Li, P.; Che, C.-M.; Peng, S.-M.; Liu, S.-T.; Zhou, Z.-Y.; Mak, T. C. W. *J. Chem. Soc., Dalton Trans.* **1993**, 189.
(7) (a) Yamamoto, Y.; Takahashi, K.; Yamazaki, H. *J. Am. Chem. Soc.* **1986**, *108*, 2458. (b) Yamamoto, Y.; Yamazaki, H. *Organometallics* **1993**, *12*, 933. (c) Tanase, T.; Kudo, Y.; Ohno, M.; Kobayashi, K.; Yamamoto, Y. *Nature* **1990**, *344*, 526. (d) Tanase, T.; Horiuchi, T.; Kobayashi, K.; Yamamoto, Y. *J. Organomet. Chem.* **1992**, *440*, 1. (e) Tanase, T.; Kawahara, K.; Ukaji, H.; Kobayashi, K.; Yamazaki, H.; Yamamoto, Y. *Inorg. Chem.* **1993**, *32*, 3682. (f) Tanase, T.; Ukaji, H.; Kudo, Y.; Ohno, M.; Kobayashi, K.; Yamamoto, Y. *Organometallics* **1994**, *13*, 1301. (g) Tanase, T.; Yamamoto, Y.; Puddephatt, R. J. *Organometallics* **1996**, *15*, 1502. (h) Tanase, T.; Nomura, T.; Fukushima, T.; Yamamoto, Y.; Kobayashi, K. *Inorg. Chem.* **1993**, *32*, 4578. (i) Tanase, T.; Fukushima, T.; Nomura, T.; Yamamoto, Y.; Kobayashi, K. *Inorg. Chem.* **1994**, *33*, 32. (j) Yamamoto, Y.; Tanase, T.; Mori, I.; Nakamura, Y. *J. Chem. Soc., Dalton Trans.* **1994**, 3191. (k) Tanase, T.; Ukaji, H.; Yamamoto, Y. *J. Chem. Soc., Dalton Trans.* **1996**, 3059.
(8) Yamamoto, Y.; Tanase, T.; Ukaji, H.; Hasegawa, M.; Igoshi, T.; Yoshimura, K. *J. Organomet. Chem.* **1995**, *498*, C23.
(9) Tanase, T.; Ukaji, H.; Igoshi, T.; Yamamoto, Y. *Inorg. Chem.* **1996**, *35*, 4114.
(10) Tanase, T.; Ukaji, H.; Igoshi, T.; Takahata, H.; Toda, H.; Yamamoto, T. To be submitted for publication.
(11) MaAuliffe, C. A.; Parish, R. V.; Randall, P. D. *J. Chem. Soc., Dalton Trans.* **1979**, 1730.
(12) Kubas, G. J. *Inorg. Synth.* **1979**, *19*, 90.
(13) Appell, R.; Geisler, K.; Scholer, H. F. *Chem. Ber.* **1979**, *112*, 648.
(14) Walborsky, H. M.; Niznik, G. E. *J. Org. Chem.* **1972**, *37*, 187.

Table 1. Crystallographic and Experimental Data for $[Pt_2Au(\mu\text{-dpmp})_2(XylNC)_2](PF_6)_3\cdot(CH_3)_2CO$ (**7**·$(CH_3)_2CO$) and $[Pt_2Ag(\mu\text{-dpmp})_2(XylNC)_2](PF_6)_3$ (**8**)

compound	**7**·$(CH_3)_2CO$	**8**
formula	$C_{85}H_{82}N_2OP_9F_{18}Pt_2Au$	$C_{82}H_{76}N_2P_9F_{18}Pt_2Ag$
fw	2355.48	2208.30
cryst system	monoclinic	monoclinic
space group	$P2_1/n$ (No. 14)	$C2/c$ (No. 15)
a, Å	15.147(3)	18.302(6)
b, Å	25.947(8)	25.056(6)
c, Å	25.759(6)	47.172(9)
β, deg	104.10(2)	99.11(3)
V, Å^3	9818	21359
Z	4	8
T, °C	23	23
D_{calcd}, g cm^{-1}	1.593	1.373
abs coeff, cm^{-1}	45.76	30.18
2θ range, deg	$3 < 2\theta < 45$	$3 < 2\theta < 45$
no. of unique data	13 149	14 373
no. of obsd data	5251 ($I > 3\sigma(I)$)	4586 ($I > 2.5\sigma(I)$)
no. of var	623	474
R^a	0.065	0.089
$R_w{}^a$	0.059	0.078

[a] $R = \sum||F_o| - |F_c||/\sum|F_o|$; $R_w = [\sum w(|F_o| - |F_c|)^2/\sum w|F_o|^2]^{1/2}$ ($w = 1/\sigma^2(F_o)$).

(N≡C), 837 (PF_6) cm^{-1}. ^{1}H NMR (acetone-d_6): δ 1.35 (s, *o*-Me), 1.49 (s, *o*-Me), 3.61, 4.44, 5.06 (m, CH_2), 6.8−8.6 (m, Ar). $^{31}P\{^1H\}$ NMR (acetone-d_6): δ −14.86 (m, $^1J_{PtP} = 2853$ Hz, 2P), −10.86 (m, 2P), −1.22 (m, $^1J_{PtP} = 2708$ Hz, 2P). UV−vis (CH_2Cl_2; λ_{max} (log ϵ)): 319 (3.98) nm. The procedures similar to that for **9** by using CuBr and CuCl instead of CuI afforded $[Pt_2CuBr(\mu\text{-dpmp})_2(XylNC)_2](PF_6)_2$ (**10**) (yield 26%) and $[Pt_2CuCl(\mu\text{-dpmp})_2(XylNC)_2](PF_6)_2$ (**11**) (yield 63%), respectively. For **10**: Anal. Calcd for $C_{82}H_{76}N_2F_{18}P_9Pt_2CuBr$: C, 46.92; H, 3.65; N, 1.33%. Found: C, 47.42; H, 3.28; N, 1.21%. IR (Nujol): 2168, 2133 (N≡C), 839 (PF_6) cm^{-1}. ^{1}H NMR (acetone-d_6): δ 1.43 (s, *o*-Me), 1.48 (s, *o*-Me), 3.61, 4.32, 4.99 (m, CH_2), 6.5−8.9 (m, Ar). $^{31}P\{^1H\}$ NMR (acetone-d_6): δ −17.17 (m, 2P), −10.97 (m, $^1J_{PtP} = 2686$ Hz, 2P), 0.87 (m, $^1J_{PtP} = 2652$ Hz, 2P). UV−vis (CH_2Cl_2; λ_{max} (log ϵ)): 316[sh] (3.91) nm. For **11**: Anal. Calcd for $C_{82}H_{76}N_2F_{18}P_9Pt_2CuCl$: C, 47.04; H, 3.66; N, 1.34%. Found: C, 46.94; H, 3.02; N, 1.29%. IR (Nujol): 2174, 2135 (N≡C), 839 (PF_6) cm^{-1}. ^{1}H NMR (acetone-d_6): δ 1.43 (s, *o*-Me), 1.50 (s, *o*-Me), 3.63, 4.36, 4.92 (m, CH_2), 6.4−8.8 (m, Ar). $^{31}P\{^1H\}$ NMR (acetone-d_6): δ −19.71 (m, 2P), −8.20 (m, $^1J_{PtP} = 2686$ Hz, 2P), 1.53 (m, $^1J_{PtP} = 2652$ Hz, 2P). UV−vis (CH_2Cl_2; λ_{max} (log ϵ)): 321 (4.00) nm.

X-ray Crystallographic Analyses of 7·$(CH_3)_2CO$, 8, 9·Et_2O, 10·Et_2O, and 11·Et_2O. The crystals used in the data collection were sealed into a glass tube capillary (0.7 mm o.d.) with a droplet of mother liquor. Crystal data and experimental conditions are summarized in Tables 1 and 2. All data were collected on a Rigaku AFC5S diffractometer equipped with graphite monochromated Mo Kα (λ = 0.710 69 Å) radiation. The cell constants were obtained from least-squares refinement of 23−25 reflections with $20 < 2\theta < 30°$. Three standard reflections were monitored every 150 reflections and showed no systematic decrease in intensity. Reflection data were corrected for Lorentz−polarization and absorption effects (ψ-scan method).

The structure of **7**·$(CH_3)_2CO$ was solved by direct methods with MITHRIL.[15] Two Pt and one Au atoms were located initially, and subsequent Fourier syntheses gave the positions of other non-hydrogen atoms. The coordinates of all hydrogen atoms except those of the solvent molecule were calculated at ideal positions with a C−H distance of 0.95 Å and were not refined. The structure was refined with the full-matrix least-squares techniques, minimizing $\sum w(|F_o| - |F_c|)^2$. Final refinement was carried out with anisotropic thermal parameters for Pt, Au, P, and F atoms and with isotropic ones for other non-hydrogen atoms. The structure of **8** was solved by Patterson method to determine the positions of two Pt and one Ag atoms. Subsequent cycles of Fourier and difference Fourier syntheses and least-squares techniques gave the positions of other non-hydrogen atoms. Final full-matrix least-squares refinement was carried out with anisotropic thermal parameters for the Pt, Ag, and P(1)−P(6) atoms and with isotropic ones for other non-hydrogen atoms. The PF_6 anions were disordered and refined with two groups having 1.0 occupancy and two with 0.5 occupancy. The structure of **9**·Et_2O was solved and refined by the procedures similar to that of **7**·$(CH_3)_2CO$ with MITHRIL. Final refinement of **9**·Et_2O was carried out with anisotropic thermal parameters for the Pt, Cu, I, P, and F atoms and with isotropic ones for other non-hydrogen atoms. The structure of **10**·Et_2O was solved by direct methods with SIR92,[16] and final refinement was carried out with anisotropic thermal parameters for the Pt, Cu, Br, P, F, O, N, and C(1)−C(6) atoms and with isotropic ones for other non-hydrogen atoms. The structure of **11**·Et_2O was solved by direct methods with MITHRIL, and final refinement was carried out with anisotropic thermal parameters for all non-hydrogen atoms.

Atomic scattering factors and values of f' and f'' for Pt, Au, Ag, Cu, I, Br, Cl, P, F, O, N, and C were taken from the literatures.[17] All calculations were carried out on a Digital VAX Station 3100 and a Silicon Graphics Indy Station with the TEXSAN Program System.[18] The perspective views were drawn by using the program ORTEP-II.[19] Compilation of final atomic parameters for all non-hydrogen atoms is supplied as Supporting Information.

Molecular Orbital Calculations. Extended Hückel molecular orbital calculations were carried out by using parameters of the Coulomb integrals and the orbital exponents taken from ref 20. For the Pt, Au, and Cu d functions, double-ξ expansions were used. The fragment analyses were performed by using program CACAO.[21] Geometrical assumptions were derived from simplifications of the crystal structures. Phosphine groups are replaced by hydride ligands to simplify the models. Pt−Pt = 2.727 Å, Pt−Au = 3.05 Å, Pt−Cu = 2.872 Å, Cu−I = 2.587 Å, Cu−Br = 2.403 Å, Cu−Cl = 2.276 Å, Pt−C = 1.950 Å, C−N = 1.15 Å, N−H = 1.01 Å, M−H = 1.700 Å. Pt−Pt−Au = 90°, Pt−Pt−Cu = 90°, Pt−Cu−X = 90°.

Results and Discussion

Preparation of $[Pt_2M(\mu\text{-dpmp})_2(XylNC)_2](PF_6)_3$ (M = Au (7), Ag (8)). The reaction of *syn*-$[Pt_2(\mu\text{-dpmp})_2(XylNC)_2](PF_6)_2$ (**1**) with $AuPF_6$, which was derived from $[AuCl(PPh_3)]$ and $NaPF_6$ *in situ*, in CH_2Cl_2 at room temperature yielded the Pt_2Au trinuclear complex formulated as $[Pt_2Au(\mu\text{-dpmp})_2(XylNC)_2](PF_6)_3$ (**7**) in 60% yield (Scheme 2). Two N≡C stretching bands were observed at 2164 and 2151 cm^{-1} in the IR spectrum. The ^{1}H NMR spectrum exhibited four singlets for *o*-methyl protons of two XylNC molecules, indicating that rotation of xylyl rings is hindered by steric effects. The $^{31}P\{^1H\}$ NMR spectrum is somewhat complicated; four sets of resonances appeared at δ −4.24, −2.31, +1.13, and +33.34 in 1:2:1:2 ratio (Figure 1). The former three were accompanied by ^{195}Pt satellite peaks with $^1J_{PtP} = 2331-2730$ Hz, whereas the latter was not. The peaks for the non-equivalent central P atoms (P_B) tentatively correspond to those at δ −4.24 and +1.13. The resonances for the P_A and P_C atoms did not so largely split. The similar Pt_2Ag cluster, $[Pt_2Ag(\mu\text{-dpmp})_2(XylNC)_2](PF_6)_3$ (**8**), was also prepared by the reaction of complex **1** with $AgPF_6$ in 70% yield (Scheme 2). The IR spectrum indicated the presence of two non-equivalent isocyanide ligands at 2178 and 2133 cm^{-1}. The ^{1}H NMR spectrum was similar to that of **7**, showing four singlets for *o*-methyl protons of two XylNC molecules. The $^{31}P\{^1H\}$

(15) Gilmore, G. J. *J. Appl. Crystallogr.* **1984**, *17*, 42

(16) Burla, M. C.; Camalli, M.; Cascarano, G.; Giacovazzo, C.; Polidori, G.; Spagna, R.; Viterbo, D. *J. Appl. Crystallogr.* **1989**, *22*, 389.

(17) (a) Cromer, D. T.; Waber, J. T. *International Tables for X-ray Crystallography*; Kynoch Press: Birmingham, England, 1974; Vol IV. (b) Cromer, D. T. *Acta Crystallogr.* **1965**, *18*, 17.

(18) *TEXSAN Structure Analysis Package*; Molecular Structure Corp.: The Woodlands, TX, 1985.

(19) Johnson, C. K. *ORTEP-II*; Oak Ridge National Laboratory: Oak Ridge, TN, 1976.

(20) (a) Hoffmann, R. *J. Chem. Phys.* **1963**, *39*, 1397. (b) Hoffmann, R.; Lipscomb, W. N. *J. Chem. Phys.* **1962**, *36*, 2179. (c) Hoffmann, R.; Lipscomb, W. N. *J. Chem. Phys.* **1962**, *36*, 3489. (d) Ammeter, J. H.; Burgi, H.-B.; Thibeault, J. C.; Hoffmann, R. *J. Am. Chem. Soc.* **1978**, *100*, 3686.

(21) Mealli, C.; Prosperpio, D. *J. Chem. Educ.* **1990**, 67, 399.

Table 2. Crystallographic and Experimental Data for $[Pt_2CuX(\mu\text{-dpmp})_2(XylNC)_2](PF_6)_2\cdot Et_2O$ (X = I (**9**·Et_2O), Br (**10**·Et_2O), Cl (**11**·Et_2O))

compound	**9**·Et_2O	**10**·Et_2O	**11**·Et_2O
formula	$C_{86}H_{86}N_2OP_8F_{12}Pt_2CuI$	$C_{86}H_{86}N_2OP_8F_{12}Pt_2CuBr$	$C_{86}H_{86}N_2OP_8F_{12}Pt_2CuCl$
fw	2220.04	2173.04	2128.59
crystal system	monoclinic	monoclinic	monoclinic
space group	$P2_1/c$ (No. 14)	$P2_1/c$ (No. 14)	$P2_1/c$ (No.14)
a, Å	15.048(4)	14.910(4)	15.037(4)
b, Å	21.922(3)	21.891(7)	22.081(6)
c, Å	27.840(3)	27.226(8)	27.449(4)
β, deg	101.89(1)	101.66(6)	101.92(2)
V, Å^3	8987	8702	8917
Z	4	4	4
T, °C	23	−95	23
D_{calcd}, g cm^{-1}	1.641	1.658	1.585
abs coeff, cm^{-1}	39.21	41.15	36.39
2θ range, deg	$3 < 2\theta < 45$	$3 < 2\theta < 45$	$3 < 2\theta < 47$
no. of unique data	12 111	11 714	13 585
no. of obsd data	4725 ($I > 3\sigma(I)$)	8435 ($I > 3\sigma(I)$)	8157 ($I > 3\sigma(I)$)
no. of var	573	619	1018
R^a	0.056	0.042	0.040
$R_w{}^a$	0.046	0.046	0.041

[a] $R = \sum||F_o| - |F_c||/\sum|F_o|$; $R_w = [\sum w(|F_o| - |F_c|)^2/\sum w|F_o|^2]^{1/2}$ ($w = 1/\sigma^2(F_o)$).

Scheme 2

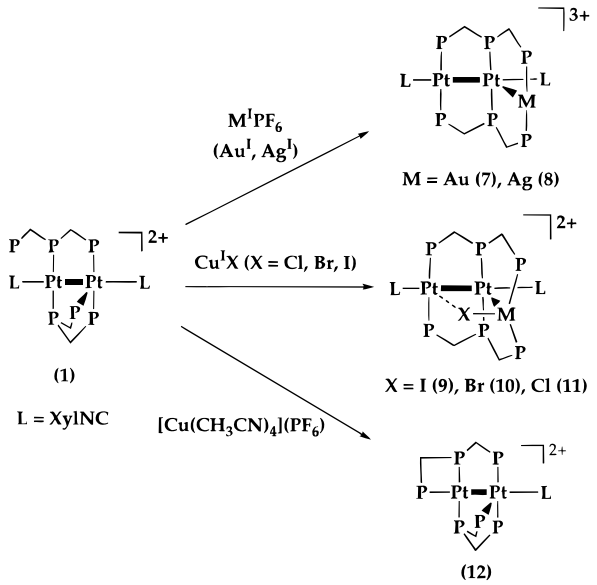

NMR spectrum was broad and prevented further detailed assignments. Complexes **7** and **8** are stable in both solid and solution states under an atmospheric condition.

Structures of $[Pt_2M(\mu\text{-dpmp})_2(XylNC)_2](PF_6)_3$ (M = Au (7), Ag (8)). The structures of **7** and **8** were determined by X-ray crystallography. The asymmetric unit of **7** contains one complex cation and three hexafluorophosphate anions, and there is no unusual interaction between the cation and the anions. An ORTEP diagram of the complex cation of **7** is illustrated in Figure 2, and some selected bond lengths and angles are summarized in Table 3. The complex cation comprises a Pt_2Au trinuclear core bridged by two dpmp ligands An Au(I) ion is trapped by two uncoordinated phosphine units in **1′** to lead to a deformed Pt−Pt···Au aggregation. The two isocyanide molecules are terminally coordinated to the Pt_2 unit in a linear array. The Pt(1)-Pt(2) and Pt(1)···Au(1) distances are 2.708(2) and 3.045(2) Å, respectively. The former is at the long end of the Pt−Pt single bonds, and the latter indicated that the interaction between the Pt(1) and Au(1) atoms is weak. The Pt···Au interatomic distance (3.045(2) Å) is quite close to that of the $d^{10}-d^8$ mixed metal dimer $[AuPt(\mu\text{-dppm})_2(CN)_2]^+$ (3.046(2) Å)[22] (dppm = bis(diphenylphosphino)methane), somewhat longer than that found in $[AuPt(\mu\text{-dppm})_2(C{\equiv}CPh)_2]^+$ (2.910(1) Å),[23] and is considerably longer than those found in

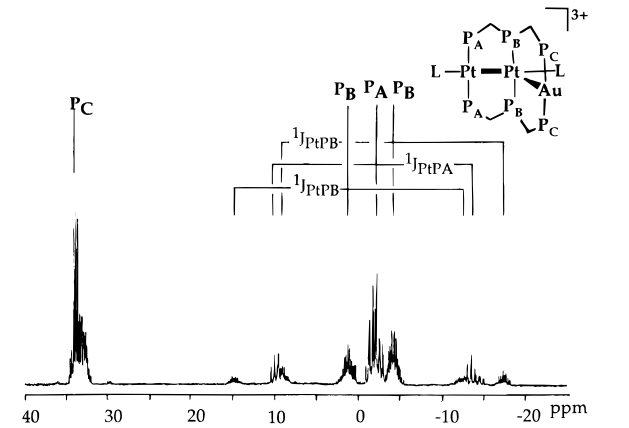

Figure 1. $^{31}P\{^1H\}$ NMR spectrum of $[Pt_2Au(\mu\text{-dpmp})_2(XylNC)_2](PF_6)_3$ (**7**) in acetone-d_6 at room temperature.

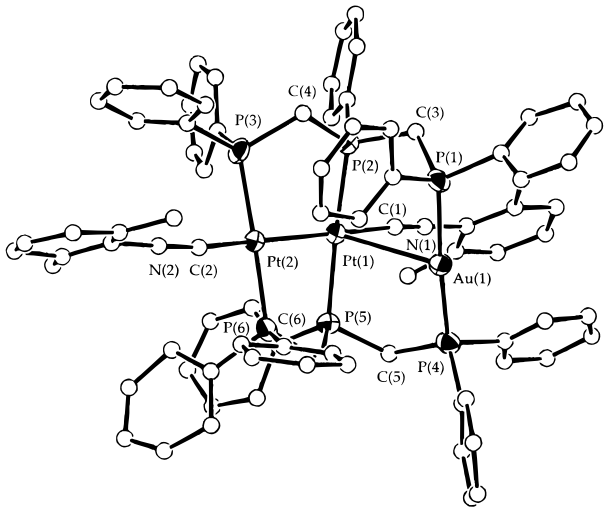

Figure 2. ORTEP diagram of the complex cation of **7**, $[Pt_2Au(\mu\text{-dpmp})_2(XylNC)_2]^{3+}$, with the atomic numbering scheme for selected atoms.

$Pt^I-Au^I-Pt^I$ A-frame type clusters, $[Pt_2(C{\equiv}C\text{-}t\text{-}Bu)_2(\mu\text{-AuI})(\mu\text{-dppm})_2]$ (av 2.659 Å),[24] $[Pt_2(\mu\text{-AuCl})(\mu\text{-dppm})_2(CN)_2]$ (av

(22) Yip, H.-K.; Che, C.-M.; Peng, S.-M. *J. Chem. Soc., Chem. Commun.* **1991**, 1626.
(23) Yip, H.-K.; Lin, H.-M.; Wang, Y.; Che, C.-M. *J. Chem. Soc., Dalton Trans.* **1993**, 2939.
(24) Manojlovic-Muir, L.; Muir, K. W.; Treurnicht, I.; Puddephatt, R. J. *Inorg. Chem.* **1987**, *26*, 2418.

Table 3. Selected Bond Distances (Å) and Angles (deg) for $[Pt_2Au(\mu\text{-dpmp})_2(XylNC)_2](PF_6)_3\cdot(CH_3)_2CO$ (**7**·$(CH_3)_2CO$)[a]

Bond Distances			
Pt(1)−Pt(2)	2.708(2)	Pt(1)···Au(1)	3.045(2)
Pt(1)−P(2)	2.326(7)	Pt(1)−P(5)	2.299(7)
Pt(1)−C(1)	2.08(2)	Pt(2)−P(3)	2.323(8)
Pt(2)−P(6)	2.278(7)	Pt(2)−C(2)	1.90(3)
Au(1)−P(1)	2.349(7)	Au(1)−P(4)	2.328(7)
N(1)−C(1)	1.12(3)	N(2)−C(2)	1.19(3)

Bond Angles			
Au(1)···Pt(1)−Pt(2)	110.68(5)	Au(1)−Pt(1)−P(2)	92.5(2)
Au(1)−Pt(1)−P(5)	83.4(2)	Au(1)−Pt(1)−C(1)	73.0(6)
Pt(2)−Pt(1)−P(2)	92.4(2)	Pt(2)−Pt(1)−P(5)	87.8(2)
Pt(2)−Pt(1)−C(1)	176.2(6)	P(2)−Pt(1)−P(5)	175.6(3)
P(2)−Pt(1)−C(1)	88.2(6)	P(5)−Pt(1)−C(1)	91.9(6)
Pt(1)−Pt(2)−P(3)	87.4(2)	Pt(1)−Pt(2)−P(6)	94.8(2)
Pt(1)−Pt(2)−C(2)	178.5(8)	P(3)−Pt(2)−P(6)	177.8(3)
P(3)−Pt(2)−C(2)	93.6(8)	P(6)−Pt(2)−C(2)	84.2(8)
Pt(1)−Au(1)−P(1)	86.9(2)	Pt(1)−Au(1)−P(4)	93.4(2)
P(1)−Au(1)−P(4)	172.9(3)	Pt(1)−C(1)−N(1)	175(2)
Pt(2)−C(2)−N(2)	168(2)	C(1)−N(1)−C(11)	177(3)
C(2)−N(2)−C(21)	175(2)		

[a] Estimated standard deviations are given in parentheses.

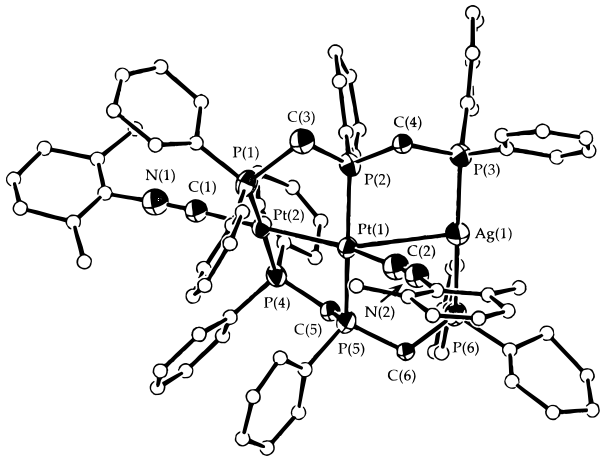

Figure 3. ORTEP diagram of the complex cation of **8**, $[Pt_2Ag(\mu\text{-dpmp})_2(XylNC)_2]^{3+}$, with the atomic numbering scheme for selected atoms.

2.641 Å),[25] and $[Pt_2(\mu\text{-AuPPh}_3)\{C_6H_4P(Ph)CH_2CH_2CH_2PPh_2\}_2]BF_4$ (av 2.710 Å),[26] which were considered as typical bonding interactions. The Pt(2)−Pt(1)···Au(1) angle is 110.68(5)°, resulting in a Y-shaped LPt_2AuL structure, which is interesting compared with the linear LPt_2PdL structure of **6** derived from the reaction of **1** with the d^{10} Pd(0) isocyanide complex.[8] In the latter case, one electron transfer from the d^{10} metal center to the d^9−d^9 diplatinum center led to a d^9−d^{10}−d^9 Pt_2Pd aggregation joined by two metal−metal covalent bonds. In the present case, however, the d^{10} Au(I) center is separated from the Pt_2 dinuclear center, leading to no typical metal−metal bonding interaction between the Au and Pt atoms. The P−M−P axes are tilted with each other with the average PPt(1)Pt(2)P and PPt(1)Au(1)P torsional angles of 25.0° and 21.2°, respectively.

The crystal structure of **8** is essentially identical to that of **7** (Figure 3 and Table 4). The Pt(1)−Pt(2) bond length of 2.657(2) Å is shorter than that found in **7**. The Pt(1)···Ag(1) distance of 3.118(3) Å is comparable to that of $[PtAgI(\mu\text{-dppm})_2(C{\equiv}CPh)_2]$ (3.146(3) Å)[27] and is longer than the Pt−Au distance in **7**, tentatively due to the lanthanide contraction and relativistic effects although the covalent radii of Au and Ag are almost identical (∼1.34 Å).[28] A comparison of structural parameters between **7** and **8** implies that the interaction between the Pt and M atoms is getting smaller; the Pt−Pt bond strength becomes stronger. These observations could suggest that the property of the Pt−Pt bond can be tuned by the additional metal ion. The Pt(2)−Pt(1)···Ag(1) angle is 136.36(8)° and the Pt(2)−Pt(1)−C(2) angle is 159.2(9)°, the terminal isocyanide on Pt(1) being deformed from a linear structure. The P(2)-Pt(1)P(5) and P(1)Pt(2)P(4) axes are considerably tilted with the average PPt(1)Pt(2)P torsional angle of 40.0°, whereas the P(2)Pt(1)P(4) and P(3)Ag(1)P(6) axes are almost parallel, the average PPt(1)Ag(1)P torsional angle being 9.3°.

Table 4. Selected Bond Distances (Å) and Angles (deg) for $[Pt_2Ag(\mu\text{-dpmp})_2(XylNC)_2](PF_6)_3$ (**8**)[a]

Bond Distances			
Pt(1)−Pt(2)	2.657(2)	Pt(1)···Ag(1)	3.118(3)
Pt(1)−P(2)	2.289(8)	Pt(1)−P(5)	2.281(9)
Pt(1)−C(2)	1.98(3)	Pt(2)−P(1)	2.32(1)
Pt(2)−P(4)	2.303(9)	Pt(2)−C(1)	1.95(3)
Ag(1)−P(3)	2.40(1)	Ag(1)−P(6)	2.405(9)
N(1)−C(1)	1.20(4)	N(2)−C(2)	1.19(4)

Bond Angles			
Ag(1)···Pt(1)−Pt(2)	136.36(8)	Ag(1)−Pt(1)−P(2)	83.4(2)
Ag(1)−Pt(1)−P(5)	90.9(2)	Ag(1)−Pt(1)−C(2)	64.1(9)
Pt(2)−Pt(1)−P(2)	82.5(2)	Pt(2)−Pt(1)−P(5)	89.2(2)
Pt(2)−Pt(1)−C(2)	159.2(9)	P(2)−Pt(1)−P(5)	160.9(3)
P(2)−Pt(1)−C(2)	98.8(9)	P(5)−Pt(1)−C(2)	95.0(9)
Pt(1)−Pt(2)−P(1)	85.6(2)	Pt(1)−Pt(2)−P(4)	93.3(2)
Pt(1)−Pt(2)−C(1)	173.3(9)	P(1)−Pt(2)−P(4)	176.0(3)
P(1)−Pt(2)−C(1)	88.2(9)	P(4)−Pt(2)−C(1)	92.7(9)
Pt(1)−Ag(1)−P(3)	91.9(2)	Pt(1)−Ag(1)−P(6)	88.0(2)
P(3)−Ag(1)−P(6)	176.9(3)	Pt(2)−C(1)−N(1)	178(2)
Pt(1)−C(2)−N(2)	165(3)	C(1)−N(1)−C(11)	176(3)
C(2)−N(2)−C(21)	173(2)		

[a] Estimated standard deviations are given in parentheses.

Preparation of $[Pt2CuX(\mu\text{-dpmp})_2(XylNC)_2](PF_6)_2$ (X = I (9), Br (10), Cl (11)). When complex **1** was treated with $[Cu(CH_3CN)_4](PF_6)$ in dichloromethane at room temperature, the dinuclear Pt(I) complex formulated as $[Pt_2(\mu\text{-dpmp})_2(XylNC)](PF_6)_2$ (**12**) (Scheme 2) was obtained in high yield (71%) instead of the hypothetical mixed metal complex $[Pt_2Cu(\mu\text{-dpmp})_2(XylNC)_2](PF_6)_3$. Compound **12** could be regarded as a product derived from removal of one isocyanide molecule from **1**. The detailed synthetic procedures and structural details will be reported elsewhere.[10] Whereas the reaction of **1** with CuI in the presence of NH_4PF_6 also led to the formation of **12**, the similar reaction in the absence of NH_4PF_6 afforded a yellow complex formulated as $[Pt_2CuI(\mu\text{-dpmp})_2(XylNC)_2](PF_6)_2$ (**9**) in 54% yield. The IR and ^1H NMR spectra indicated the presence of two kinds of terminal isocyanide ligands at $\nu_{N\equiv C}$ = 2170 and 2133 cm^{-1} and δ 1.35 and 1.49 for *o*-methyl protons, respectively. In the $^{31}P\{^1H\}$ NMR spectrum, three sets of resonances were observed at δ −14.86, −10.96, and −1.22 in a ratio of 1:1:1 (Figure 4a). The middle multiplet (δ −10.86) was rather broad and did not have satellite peaks due to one-bond coupling to ^{195}Pt, corresponding to the terminal P atoms coordinated to the Cu atom (P_C). The other two (δ −14.86, 1.22) appeared with ^{195}Pt satellite peaks ($^1J_{PtP}$ = 2708−2853 Hz), the former being assigned to the terminal P atoms attached to the Pt atom (P_A) and the latter to the central P atoms bound to the Pt atom (P_B), on the basis of their multiplicity and chemical shifts. The analogous complexes, $[Pt_2CuX(\mu\text{-dpmp})_2(XylNC)_2](PF_6)_2$ (X = Br (**10**), Cl (**11**)) were obtained by similar reactions using CuBr and CuCl as a copper source. The IR,

(25) Toronto, D. V.; Balch, A. L. *Inorg. Chem.* **1994**, *33*, 6132.
(26) Bennett, M. A.; Berry, D. E.; Beveridge, K. A. *Inorg. Chem.* **1990**, *29*, 4148.
(27) McDonald, W. S.; Pringle, P. G.; Shaw, B. K. *J. Chem. Soc., Chem. Commun.* **1982**, 861.
(28) Pauling, L. *In The Nature of the Chemical Bond*, 3rd ed.; Cornell University Press: Ithaca, NY, 1960.

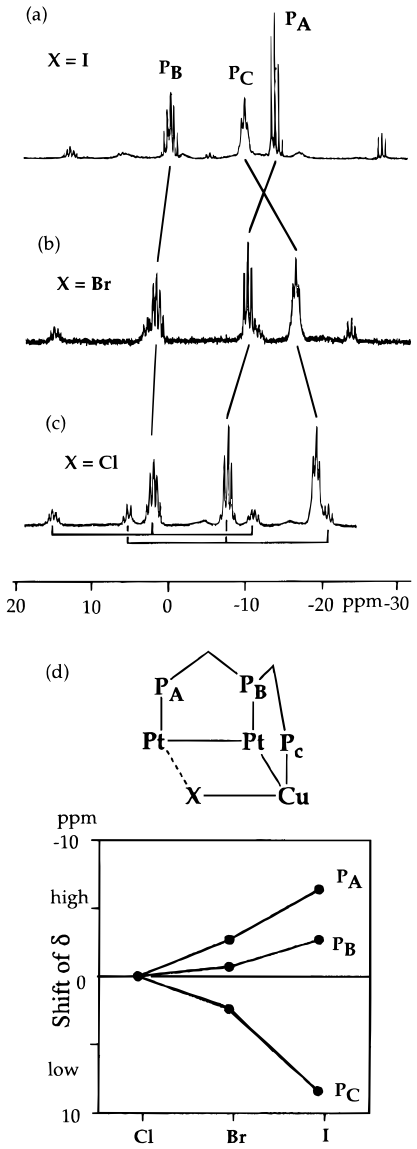

Figure 4. $^{31}P\{^1H\}$ NMR spectrum of (a) $[Pt_2CuI(\mu\text{-dpmp})_2(XylNC)_2](PF_6)_2$ (**9**), (b) $[Pt_2CuBr(\mu\text{-dpmp})_2(XylNC)_2](PF_6)_2$ (**10**), and (c) $[Pt_2CuCl(\mu\text{-dpmp})_2(XylNC)_2](PF_6)_2$ (**11**) in acetone-d_6 at room temperature. (d) Shifts of ^{31}P resonances (ppm) referenced to those of **11**. Cl, Br, and I of the horizontal axis indicate compounds **11**, **10**, and **9**, respectively.

^1H NMR, and $^{31}P\{^1H\}$ NMR spectroscopic features were quite close to those of **9** (X = I). Complexes **9**−**11** are stable in both solid and solution states under atmospheric conditions.

Structures of $[Pt_2CuX(\mu\text{-dpmp})_2(XylNC)_2](PF_6)_2$ (X = I, Br, Cl). The solid state structures of **9**−**11** were determined by X-ray crystallographic analyses to reveal that complexes **9**−**11** are isomorphous to each other. The unit cell involves four complex cations, eight PF_6^- anions, and four solvated diethyl ether molecules without unusual interaction between them. ORTEP plot of the complex cation of **10** (X = Br) is illustrated in Figure 5 as a representative one, and selected bond lengths and angles are listed in Table 5. The complex cation consists of two Pt atoms and one Cu atom bridged by two dpmp ligands and has a pseudo C_s symmetry with a mirror plane comprising the Pt_2CuBr atoms. The Pt_2CuBr assembly forms a rhombic structure with the Pt(1)−Pt(2), Pt(2)···Cu(1), Cu(1)−Br(1), and Pt(1)···X(1) distances being 2.7180(5), 2.857(1), 2.412(2), and 3.088(1) Å, respectively (Figure 5b). The Pt−Pt bond length in **10** is slightly longer than those found in **7** and **8**. Although the Pt···Cu interatomic distance in **10** (2.857(1) Å) is considerably shorter than the corresponding values of Pt···Au (3.045(2) Å (**7**)) and Pt···Ag (3.118(3) Å (**8**)) distances,

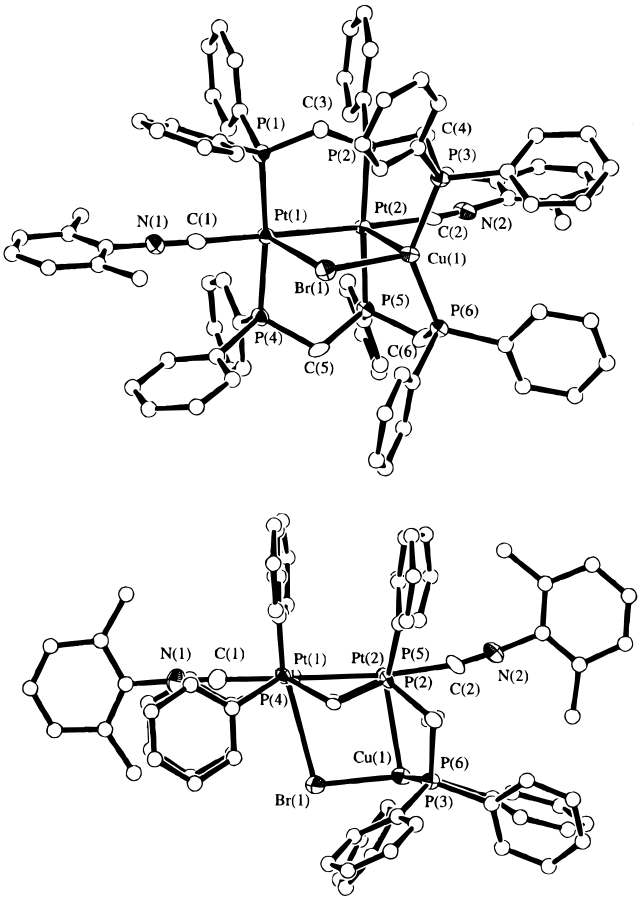

Figure 5. (a, top) ORTEP diagram of the complex cation of **10**, $[Pt_2CuBr(\mu\text{-dpmp})_2(XylNC)_2]^{2+}$, with the atomic numbering scheme for selected atoms. (b, bottom) ORTEP diagram of the complex cation of **10** viewed down vertically to the Pt_2CuBr plane.

no typical bonding interaction between the Pt and Cu atoms is estimated on the basis of small covalent radius of Cu(I) (∼1.17 Å).[28] Each Pt atom is terminally coordinated by a isocyanide molecule, and the coordination planes around the two Pt atoms are almost parallel to lead a side-by-side type dinuclear structure. The average bond distance of the P atoms to the Pt(2) atom (2.283(3) Å) is shorter than that to the Pt(1) atom (2.296(3) Å). In contrast, the bond distance of XylNC to the Pt(2) atom (2.01(1) Å) is longer than that to the Pt(1) atom (1.94(1) Å). The XylNC ligand on the Pt(2) atom is deformed from the LPtPtL (L = XylNC) axis (Pt(1)−Pt(2)−C(2) = 170.5(9)°), probably due to the steric repulsion with the Cu fragment. The Cu(1) atom is ligated by two P atoms and a bromide anion to form a distorted three-coordinate structure, a sum of the angles P(3)−Cu(1)−P(6), P(3)−Cu(1)−Br(1), and P(6)−Cu(1)−Br(1) being 358.88°. The coordination plane around the Cu atom is approximately parallel to the Pt_2 coordination plane, so-called face-to-face arrangement. The Pt(2)···Cu(1)−Br(1) angle (85.94(4)°) is interestingly less than 90°, resulting in a relatively short interatomic distance between the Pt(1) and Br(1) atoms (3.088(1) Å). The Pt(1)···X(1) distances of **9**−**11** fall within the narrow range (3.088(1)−3.130(2) Å), independent of the Cu(1)−X(1) bond lengths (2.276(3)−2.597(2) Å). These short contacts between the halides and the terminal Pt atoms are not observed in $[Pt_3Cl_2(\mu\text{-dpmp})_2(XylNC)_2]^{2+}$ (**5**), which was prepared by the reaction of **1** with d^8 Pt(II) species and has a face-to-face structure similar to those of complexes **9**−**11**, the distance between the Pt(1) and Cl(2) atoms being 4.499(9) Å (Figure 6).[9] Other structural features of **9** and **11** are the same as those found in **10** (Table 5).

A comparison of the $^{31}P\{^1H\}$ NMR spectra for complexes **9**−**11** is shown in Figure 4. When the halide anion was changed

Table 5. Structural Parameters for $[Pt_2CuX(\mu\text{-dpmp})_2(XylNC)_2](PF_6)_2\cdot Et_2O$ (X = I (**9**·Et_2O), Br (**10**·Et_2O), Cl (**11**·Et_2O)[a]

complexes	**9** (X = I)	**10** (X = Br)	**11** (X = Cl)
	Bond Distances (Å)		
Pt(1)−Pt(2)	2.715(1)	2.1780(5)	2.7273(8)
Pt(1)−P(1)	2.303(5)	2.294(3)	2.303(3)
Pt(1)−P(4)	2.315(5)	2.298(3)	2.302(3)
Pt(1)−C(1)	1.90(2)	1.94(1)	1.95(1)
Pt(1)···X(1)	3.130(2)	3.088(1)	3.111(3)
Pt(2)−P(2)	2.293(5)	2.282(2)	2.292(3)
Pt(2)−P(5)	2.288(5)	2.285(3)	2.289(3)
Pt(2)−C(2)	2.06(1)	2.01(1)	2.01(1)
Pt(2)···Cu(1)	2.863(2)	2.857(1)	2.872(1)
Cu(1)−X(1)	2.597(2)	2.412(2)	2.276(3)
Cu(1)−P(3)	2.267(5)	2.254(3)	2.260(3)
Cu(1)−P(6)	2.296(5)	2.276(3)	2.282(3)
	Bond Angles (deg)		
Pt(2)−Pt(1)−P(1)	92.5(1)	92.81(6)	92.75(7)
Pt(2)−Pt(1)−P(4)	93.1(1)	92.48(6)	92.81(7)
Pt(2)−Pt(1)−C(1)	178.1(5)	179.1(3)	178.6(3)
P(1)−Pt(1)−P(4)	169.7(2)	172.74(9)	173.4(1)
P(1)−Pt(1)−C(1)	88.8(5)	87.0(3)	87.2(3)
P(4)−Pt(1)−C(1)	85.5(5)	87.6(3)	87.1(3)
Pt(2)-Pt(1)···X(1)	80.48(3)	76.50(2)	74.22(5)
Pt(1)−Pt(2)−P(2)	92.2(1)	91.69(6)	91.64(7)
Pt(1)−Pt(2)−P(5)	91.7(1)	91.84(6)	91.68(7)
Pt(1)−Pt(2)−C(2)	173.1(4)	173.1(3)	172.7(3)
P(2)−Pt(2)−P(5)	174.1(2)	173.96(9)	173.45(9)
P(2)−Pt(2)−C(2)	87.6(5)	88.8(3)	98.2(3)
P(5)−Pt(2)−C(2)	89.0(5)	88.3(3)	88.3(3)
Pt(1)−Pt(2)···Cu(1)	97.96(5)	98.09(3)	97.74(3)
X(1)−Cu(1)−P(3)	114.2(1)	114.93(8)	114.1(1)
X(1)−Cu(1)−P(6)	108.0(1)	106.95(8)	108.3(1)
P(3)−Cu(1)−P(6)	136.5(2)	137.0(1)	136.5(1)
Pt(2)···Cu(1)−X(1)	87.75(7)	85.94(4)	85.92(8)
Cu(1)−X(1)···Pt(1)	93.92(6)	99.20(4)	102.0(1)

[a] Estimated standard deviations are given in parentheses.

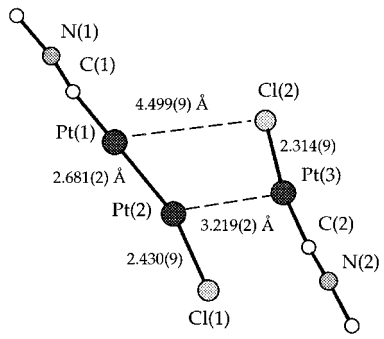

Figure 6. Structure of the metal centers of **5**, $[Pt_3Cl_2(\mu\text{-dpmp})_2(XylNC)_2](PF_6)_2$.

from Cl^- to Br^- and I^-, the resonances corresponding to the P_A and P_c atoms significantly moved to high and low fields, respectively, as depicted in Figure 4d, while that for the P_B atom did not so much. This spectral change could suggest that the halide anion interacted with the terminal Pt atom as well as the Cu center, and thus the rhombic Pt_2CuX structure is essentially retained even in the solution state.

Molecular Orbital Calculations. In order to understand the basic electronic interactions between the diplatinum core and the group 11 metal ions in **7**−**11**, extended Hückel MO calculations were carried out.

The interaction diagram for a model compound $[Pt_2AuH_6(HNC)_2]^{3-}$ (Pt−Pt−Au = 90°, **13**) in terms of the diplatinum complex $[Pt_2H_4(HNC)_2]^{2-}$ and the Au unit $[AuH_2]^-$ is shown in the left side of Figure 7. The phosphine groups are replaced by hydride ligands with M−H interactions of 1.70 Å to simplify the MO interactions; the molecular orbitals are essentially the same as those with PH_3 groups. The HOMO of

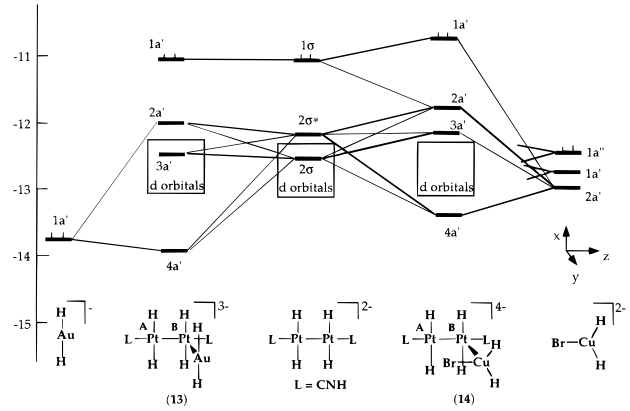

Figure 7. Interaction diagrams for $[Pt_2AuH_6(HNC)_2]^{3-}$ (**13**) in terms of $[Pt_2H_4(HNC)_2]^{2-}$ and $[AuH_2]^-$ fragments (left) and $[Pt_2CuBrH_6(HNC)_2]^{4-}$ (**14**) in terms of $[Pt_2H_4(HNC)_2]^{2-}$ and $[CuBrH_2]^{2-}$ fragments (left).

13 (1a′) is exclusively derived from the HOMO of the diplatinum unit which involves a σ bonding interaction of hybridized d orbitals of the two Pt atoms. The highest occupied orbital of the Au(I) unit, a hybridized d orbital, only slightly interacts with low-lying occupied d orbitals of the $Pt(I)_2$ unit (2σ, 2σ*), resulting in almost no bonding interaction between the Au(I) and $Pt(I)_2$ fragments. The overlap population (OP) between two Pt atoms is 0.391, which is the normal value for a Pt−Pt σ-bond, whereas that between the Pt_B and Au atoms is 0.049, showing a slight bonding character. When the Pt_A−Pt_B−Au angle is expanded from 90°, the 4a′ orbital of **13**, derived from a bonding interaction between d_{hy} orbitals of Pt_B and Au atoms, is destabilized by repulsive interactions with the d_{yz} orbital of the Pt_B atom. The OP between Pt_B and Au decreases and that between Pt_A and Pt_B increases with the expansion of Pt_A−Pt_B−Au angle.

The interaction diagram for $[Pt_2CuBrH_6(CNH)_2]^{4-}$ (Pt_A−Pt_B−Cu = 90°, Pt−Cu−Br = 90°; **14**) in terms of the diplatinum complex and the $[CuBrH_2]^{2-}$ trigonal fragment is illustrated in the right side of Figure 7. The occupied 2a′ orbital of the Cu fragment consists of the d_{yz} orbital of Cu and the p_y orbital of Br in a repulsive way and mainly interacts with the low-lying occupied 2σ* orbital of the Pt_2 unit to produce bonding and antibonding molecular orbitals (2a′ and 4a′). Although no typical bond is estimated, the slight bonding nature between Pt_A and Br and between Pt_B and Cu is assumed on the basis of the corresponding OP of 0.044 and 0.060, respectively. The 4a′ orbital of **14** might be responsible for this interaction.

Conclusion. In this study, a monovalent group 11 metal ion (Au(I), Ag(I), or Cu(I)), which has a d^{10} configuration, was readily incorporated into the Pt_2 core, leading to heterotrimetallic Pt_2M complexes **7**−**11**. The structures of **7**−**11** are interestingly compared with the linearly ordered Pt−Pt−M structure of **3** and **4**, which were prepared by the reaction of **1** with d^{10} Pt and Pd fragments. These reactions could be useful in strategic synthesis of heterotrinuclear complexes, where the cluster core could be tuned by the choice of the additional metal.

Acknowledgment. This work was partially supported by a Grant-in-Aid for Scientific Research from the Ministry of Education of Japan.

Supporting Information Available: Tabulations of crystallographic data, and positional and thermal parameters for **7**·$(CH_3)_2CO$, **8**, **9**·Et_2O, **10**·Et_2O, and **11**·Et_2O and figures of ORTEP plots of **9** and **11** (51 pages). Ordering information is given on any current masthead page.

IC960771X